Ciemat 723
Sp ISSN 614-087-X

Papers presented at the FOURTEENTH INTERNATIONAL CONFERENCE ON PLASMA PHYSICS AND CONTROLLED NUCLEAR FUSION RESEARCH
Organización Internacional de la Energía Atómica
Würzburg, Alemania
30 Septiembre- 7 Octubre 1992

CENTRO DE INVESTIGACIONES
ENERGETICAS, MEDIOAMBIENTALES Y TECNOLOGICAS

MADRID, 1994

CLASIFICACION DOE Y DESCRIPTORES:

700310
PLASMA CONFINEMENT
THERMONUCLEAR DEVICES
HELIAC STELLARATORS
TORSATRON STELLARATORS
TOKAMAK DEVICES
THERMONUCLEAR REACTIONS
THERMONUCLEAR REACTORS

Toda correspondencia en relación con este trabajo debe dirigirse al Servicio de Información y Documentación, Centro de Investigaciones Energéticas, Medioambientales y Tecnológicas, Ciudad Universitaria, 28040-MADRID, ESPAÑA.

Las solicitudes de ejemplares deben dirigirse a este mismo Servicio.

Los descriptores se han seleccionado del Thesauro del DOE para describir las materias que contiene este informe con vistas a su recuperación. La catalogación se ha hecho utilizando el documento DOE/TIC-4602 (Rev. 1) Descriptive Cataloguing On-Line, y la clasificación de acuerdo con el documento DOE/TIC.4584-R7 Subject Categories and Scope publicados por el Office of Scientific and Technical Information del Departamento de Energía de los Estados Unidos.

Este trabajo se ha recibido para su impresión en Febrero 1.993

Depósito Legal nº M-19031-1993
ISBN 84-7834-196-X
ISSN 614-087-X
NIPO 238-94-008-X

IMPRIME CIEMAT

INDEX

EQUILIBRIUM AND STABILITY PROPERTIES OF THE FOUR PERIOD HELIAC TJ-II

C. ALEJALDRE, L. GARCIA, J.A. JIMENEZ, A. LOPEZ-FRAGUAS,
A. SALAS, A. VARIAS
Asociación Euratom-CIEMAT para fusión,
Madrid, Spain

Abstract

EQUILIBRIUM AND STABILITY PROPERTIES OF THE FOUR PERIOD HELIAC TJ-II.

The equilibrium and stability properties of the flexible Heliac TJ-II under construction in Spain are described. Equilibrium is studied by using the full 3-D equilibrium code PIES that permits the evolution of islands to be followed as the pressure is increased. The stability analysis was conducted for Mercier, ballooning and dissipative trapped electron modes.

1. EQUILIBRIUM STUDIES

It has long been recognized that finite aspect ratio, high rotational transform heliacs could develop equilibrium problems at finite pressure owing to the beating of the pressure induced toroidal Shafranov shift with helical harmonics, but traditional production equilibrium codes such as the 3-D VMEC assume nicely nested flux surfaces [1] and hence cannot account for these effects directly. However, there are now some new 3-D codes that are not subject to the restriction of nested magnetic surfaces. One of these is PIES [2], which determines MHD equilibrium configurations by direct integration along the field lines and whose predictions have been compared with those of VMEC in cases without islands, with very good agreement [3].

The four period TJ-II is a device that is particularly well adapted to studying the evolution of the magnetic islands as the pressure is increased, because of its flexibility and its small shear. It is designed to have nearly shearless configurations with the rotational transform ranging from 0.96 to 2.48. Therefore it can, and will normally, be operated in iota windows free of low order resonances, but one can also use this flexibility to generate large islands inside the plasma. We are now conducting a systematic study of some special configurations with large islands, using the PIES code. These configurations are, of course, exceptional in the sense that they will not occur under normal operational conditions but they are nevertheless inside the range of operation. Specifically, we are studying configurations such that the rotational transform per period takes the value 1/3 somewhere inside the plasma, and therefore is close to 1/3 over the entire volume of the plasma, because of the small shear. Typically, the rotational transform per period varies between 0.331 at the magnetic axis

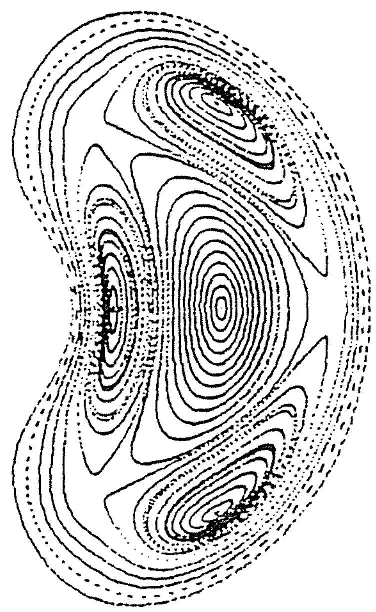

FIG. 1. Vacuum flux surfaces with the 1/3 rational value inside the rotational transform profile.

and 0.342 at the plasma boundary. As should be expected, there is a large third order island (Fig. 1).

We first consider the zero pressure case without plasma currents. In this case the structure of the magnetic field can be obtained by following the field lines of the magnetic field created by the currents in the external coils (we neglect the effect of the vacuum chamber wall and other conducting parts of the apparatus). These external currents are chosen so that we obtain the kind of configuration mentioned above, with an appropriate bean shaped cross-section for the plasma boundary. This boundary is given as an input to the PIES code. In this calculation, we assume that both the pressure and the current density are constant inside the islands and that they are continuous across the separatrices. The choice of the number of Fourier modes to be used by the code is very important. In most of our initial runs we had:

$$0 \le m \le 5$$

$$-10 + m \le n/N \le 10 + m$$

where m is the poloidal number and n/N is the toroidal number per period. This non-rectangular mode selection is chosen to take advantage of the approximate helical symmetry. The fundamental resonant term, $m = 3$, $n/N = 1$, is selected, but not the higher order terms $m = 3k$, $n/N = k$, with $k > 1$. With this mode selection, the general structure of the magnetic field given by PIES agreed reasonably well with that obtained from the currents in the external coils, with the shape and the size of the island fairly well reproduced. But there is one aspect in which the agreement was quite poor: the distribution of the magnetic surfaces inside the island. PIES gave surfaces pressing inwards inside the island, while the field created by the coils gave surfaces pressing outwards. On the other hand, another run with

$$0 \le m \le 7$$

$$-10 + m \le n/N \le 10 + m$$

which includes the resonant term $m = 6$, $n/N = 2$ as well as the fundamental term, $m = 3$, $n/N = 1$, yields the correct structure inside the island [4].

In the case of finite pressure the same plasma boundary as for the zero pressure case was used. A series of runs with different values of central beta and with the above mentioned $0 \le m \le 5$ mode selection seemed to indicate that the central width of the island decreases with increasing beta, until the island splits when $\beta(0) = 6 \times 10^{-4}$. But from some recent runs with the $0 \le m \le 7$ mode selection it appears that either there is no splitting or the splitting takes place at much higher pressures. At $\beta(0) = 1 \times 10^{-3}$ only a slight narrowing of the island is observed. More work is under way to provide a better understanding of the island evolution when the pressure increases.

2. STABILITY STUDIES

2.1. Ballooning modes

Ballooning modes are pressure driven instabilities, strongly localized in 'bad curvature' regions of the confining magnetic field that limit the achievable pressure in tokamaks. In stellarators with iota profile gradients opposite to tokamaks, it was widely believed that Mercier rather than ballooning modes were the limiting instabilities to the maximum β achievable. However, recent studies have shown that, at least in some class of stellarators, ballooning modes are, like in tokamaks, the limiting instabilities [5]. In this paper a study attempting to find out what effect, if any, ballooning modes have on the previously obtained β limits for the Heliac TJ-II under construction at CIEMAT [6] is presented. After obtaining a TJ-II equilibrium with the VMEC code, we changed it to a Boozer co-ordinate system to solve the ballooning equation. The strong indentation of the bean shaped magnetic surfaces of the TJ-II and the pronounced helicity of its magnetic axis required a great number of modes (138) to correctly describe its magnetic surfaces in a Fourier expansion:

$$R(s, \theta, \xi) = \sum R_{mn}(s) \cos (m\theta - n\xi)$$

$$Z(s, \theta, \xi) = \sum Z_{mn}(s) \sin (m\theta - n\xi)$$

Typically, $m \le 6$, $-12 \le n \le 12$ were needed to obtain, with VMEC, equilibria that correctly reproduced the vacuum magnetic surfaces and magnetic properties such as iota profile and magnetic well that were previously obtained from a field line following code. This large number of toroidal and poloidal modes becomes even larger when we try to describe the equilibrium in Boozer co-ordinates needed for the stability analysis. For a correct reconstruction of the magnetic surfaces more than 750 modes were needed for a TJ-II configuration, characterized by $\langle\beta\rangle \approx 2\%$, and even with this number of modes for the most external surfaces the reconstruction, when compared in detail with the original VMEC magnetic surfaces, was not good enough. The number of modes needed for a satisfactory reconstruction grows with β, making it more difficult, from a numerical point of view, to obtain a good representation of the surfaces as β increases. This problem restricted our study to configurations with β values such that the surfaces were well reconstructed and therefore not all cases previously considered could be analysed. By using these equilibria, the ballooning equation

$$\frac{\partial}{\partial\zeta}\,\alpha(s,\,\xi)\,\frac{\partial}{\partial\zeta}\,\Psi + D(s,\,\zeta)\Psi = \Gamma^2\, b(s,\,\zeta)\Psi$$

was solved in Boozer co-ordinates, where the bending term α is given by

$$\alpha(s,\,\zeta) = (1/g^{ss})\,\{1 + [(\Phi'\iota' g^{ss}/B)\zeta + (-Ig_{\theta s} - Jg_{\zeta s})/(\sqrt{g}B)]^2\}$$

and the driving term D is given by

$$\begin{aligned} D(s,\,\zeta) = & -\{p'\iota'/(\Phi'[J\chi' - I\Phi'])\}(-I\partial\sqrt{g}/\partial\theta \\ & -J\partial\sqrt{g}/\partial\zeta)\zeta + (1/\Phi')^2\{\sqrt{g}p'^2/B^2 - p'\partial\sqrt{g}/\partial s \\ & + (p'/B^2)(J\chi'' - I\Phi'') + (p'/B)^2(\sqrt{g} - V') \\ & + p'\sqrt{g}\, B_s\, \vec{B}\cdot\nabla\sqrt{g}(1/[J\chi' - I\Phi'])\} \end{aligned}$$

and in this co-ordinate system the term $b(s,\,\zeta)$ is written as:

$$b(s,\,\zeta) = (2/\beta_0)\{\sqrt{g}\,p^2/(\Phi' A^2)\}\,\alpha(s,\,\zeta)$$

Figure 2 shows the stabilizing bending term α and the driving term D for a TJ-II configuration that is stable to ballooning modes. Notice the very different scales in both plots. Figure 3 shows the strongly localized eigenfunction obtained from the ballooning equation in an unstable case.

We have applied this procedure to a shearless TJ-II configuration characterized by $\iota(0)M \approx 0.30$ and a vacuum magnetic well of about 1.3%. Our results, summarized in Fig. 4, indicate that, for this configuration, ballooning and Mercier modes impose similar limits on the achievable β values although numerical problems in the convergence to Boozer co-ordinates limit the confidence in the results to average

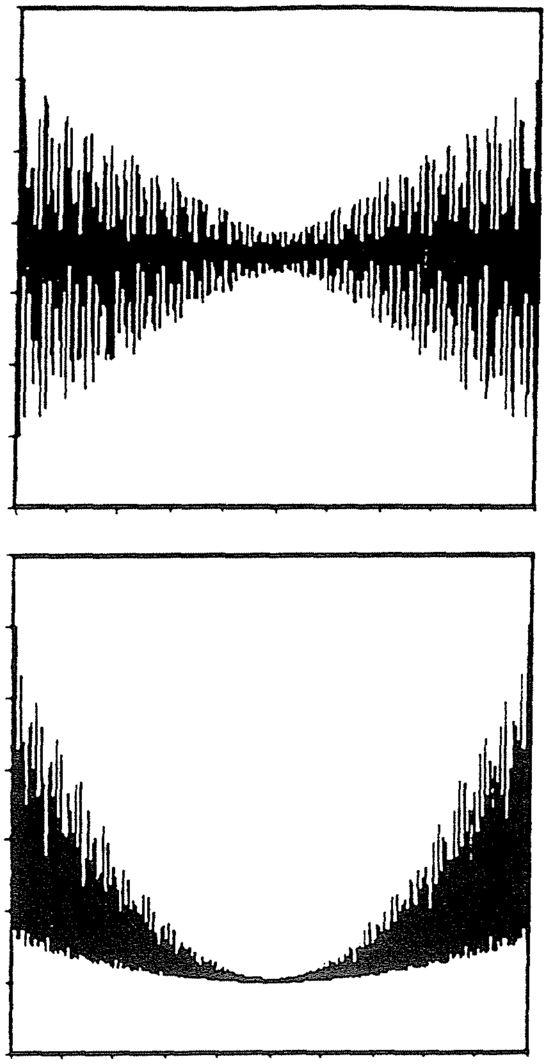

FIG. 2. Variation of driving term (above) and stabilizing term α along a field line.

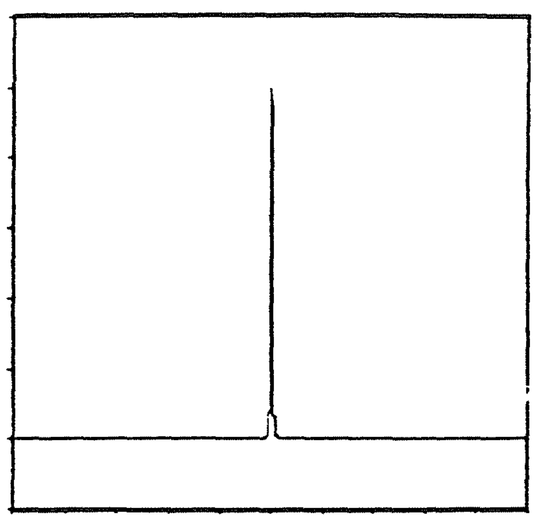

FIG. 3. Eigenfunction of the ballooning equation in an unstable TJ-II configuration showing the localization of the ballooning mode.

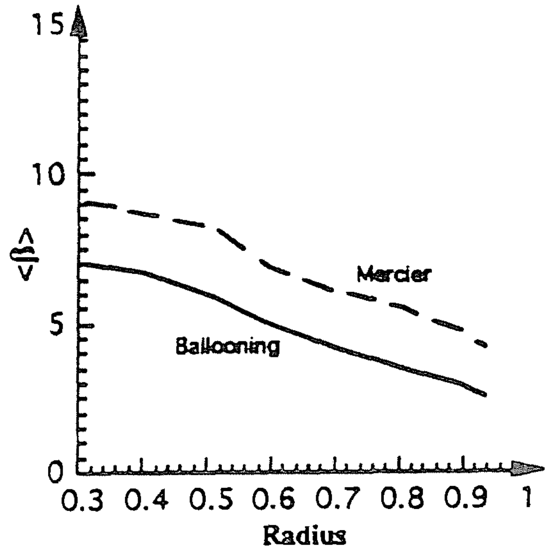

FIG. 4. Maximum β values calculated for a TJ-II configuration with Mercier criterion and ballooning equation versus minor plasma radius.

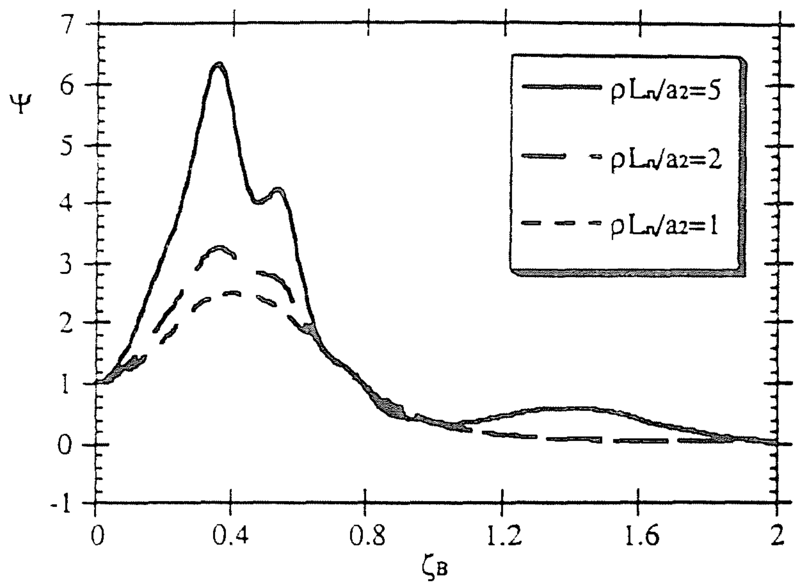

FIG. 5. Eigenfunctions at $\rho = 0.683a$, for $\omega_n = 10$.

$\beta \approx 2\%$. To clarify this point, numerical and analytical studies of the Mercier criterion and ballooning modes are under way.

2.2. DTEM

To study the dissipative trapped electron mode in TJ-II, we follow the formalism developed by Antonsen et al. [7]. It is formulated in the ballooning representation, and the drift wave problem is posed as an eigenvalue equation along a magnetic field line. The change in frequency due to the non-adiabatic electron contribution is

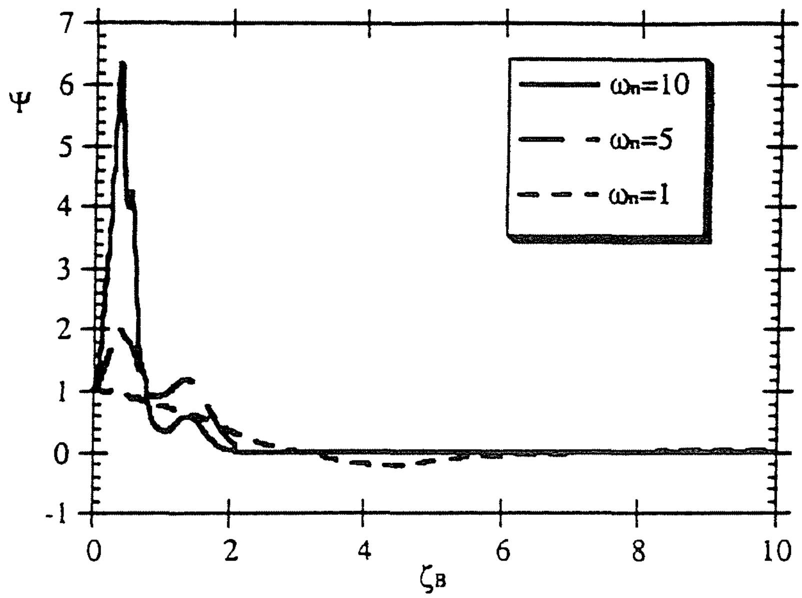

FIG. 6. Eigenfunctions at $\rho = 0.683a$, for $\rho L_n/a^2 = 5$.

calculated perturbatively [8]. We have only considered low β TJ-II equilibria. We limit the calculations to the plasma core and to regions in the parameter space where localized solutions can exist. We solve the ballooning equation for only one field line starting at half field period. The relevant parameters are ω_n and $\rho L_n/a^2$, where ω_n is the ratio of electron diamagnetic to sound frequency, ρ/a the normalized radius, L_n the electron density scale length and a the minor radius.

In Fig. 5, we plot the eigenfunctions for different values of the parameter $\rho L_n/a^2$. The configuration is one of the deep well scan with peak beta equal to 1.33%. The flux surface is located at a radius of 0.683a, and the parameter ω_n is set equal to 10. As the gradient of the density decreases, the mode changes from a helically induced to a toroidicity induced mode. The change in the eigenfunction with ω_n is illustrated in Fig. 6. The electron density scale length in 5 for the three cases. The eigenfunction becomes more localized as ω_n increases.

ACKNOWLEDGEMENTS

The authors would like to thank B.A. Carreras, N. Dominguez, S. Hirshman and A. Reiman for valuable discussions and, in particular, for providing some of the codes used in this study.

REFERENCES

[1] HIRSHMAN, S.P., VAN RIJ, W.I., MERKEL, P., Comput. Phys. Commun. 43 (1986) 157.

[2] REIMAN, A.H., GREENSIDE, H.S., J. Comput. Phys. 75 (1988) 423–443; GREENSIDE, H., REIMAN, A.H., SALAS, A., J. Comput. Phys. 81 (1988) 102–136.

[3] JOHNSON, J.L., MONTICELLO, D.A., REIMAN, A.H., SALAS, A., FRAGUAS, A.L., HIRSHMAN, S.P., Comparison of ATF and TJ-II stellarator equilibria as computed by the 3-D VMEC and PIES code, paper read at 14th Int. Conf. Numerical Simulation of Plasmas, Annapolis, USA (1991).

[4] BERK, H.L, ROSENBLUTH, M.N., SHOHET, J.L., Phys. Fluids **26** (1983) 2616.

[5] NÜHRENBERG, J., ZILLE, R., Ballooning stability optimization of Helias equilibria, paper read at Sherwood Theory Conf. San Antonio, Texas (1989) 1D4.

[6] VARIAS, A., et al., Nucl. Fusion **30** (1990) 2597.

[7] ANTONSEN, T.A., LANE, B., Phys. Fluids **23** (1980) 1205.

[8] DOMINGUEZ, N., CARRERAS, B.A., LYNCH, V.E., DIAMOND, P.H., Phys. Fluids B **4** (1992) 2894.

TURBULENCE, TRANSPORT AND ANOMALOUS ION HEATING STUDIES IN THE TJ-I TOKAMAK

C. HIDALGO, C. PARDO, B. ZURRO, A. RODRIGUEZ-YUNTA,
M.A. PEDROSA, R. BALBIN, B. BRAÑAS, F. CASTEJON,
T. ESTRADA, I. GARCIA-CORTES, L. GARCIA, A.P. NAVARRO,
M. LINIERS, E. DE LA LUNA, M.A. OCHANDO, J. SANCHEZ,
F.L. TABARES, J. VEGA, TJ-I TEAM
Asociación Euratom–CIEMAT para fusión,
Madrid, Spain

Abstract

TURBULENCE, TRANSPORT AND ANOMALOUS ION HEATING STUDIES IN THE TJ-I TOKAMAK.

Turbulence, transport and anomalous ion heating studies have been performed in the TJ-I tokamak. Evidence of substantial edge temperature fluctuations which are in phase close to opposition with the corresponding density fluctuations has been found. This result suggests the possible role of radiation in determining edge fluctuation levels. Radial electric fields, naturally occurring and externally applied at the plasma edge, induce changes in edge and global plasma parameters. In the plasma core region, the transport coefficients that govern particle and electron heat transport are similar in steady state and pulse propagation experiments. The particle pinch is close to the neoclassical pinch and there is no evidence of a significant heat pinch. Measurements of proton and impurity temperature profiles from spectral line widths have shown that the influence of non-thermal velocity fluctuations due to stochastic fields should be assumed to account for the observed impurity temperatures.

1. INTRODUCTION

Interest in the plasma edge has recently been intensified because of clear evidence that the plasma confinement properties depend on how the plasma edge is treated. A comparison between the level of temperature, potential and density fluctuations and their relative phases can provide key information on the basic mechanisms controlling edge turbulence in tokamaks and stellarators. Furthermore, an improvement of our understanding of the interrelation between edge electric fields and plasma behaviour has become a key issue in fusion research.

The simplest approach to flux balance analysis is done in steady state conditions. However, this method can only determine a limited number of transport coefficients. A perturbative experiment, such as sawtooth heat pulse propagation, can provide both the diagonal and off-diagonal transport coefficients. A comparison between steady state and perturbative studies can provide us with a better understanding of the transport mechanisms.

Finally, understanding the influence of turbulence on the spectral line width of different ions can help us to interpret the observed anomalous ion heating more satisfactorily. The present paper is organized as follows:

The experimental details are given in Section 2. The influence of atomic physics mechanisms and electric fields on edge turbulence is discussed in Section 3. Transport studies using steady state and perturbative methods are compared with each other in Section 4. The possible role of non-thermal velocity fluctuations in anomalous impurity heating is discussed in Section 5. Finally, a summary of the conclusions is presented in Section 6.

2. EXPERIMENTAL

TJ-I is an ohmically heated tokamak ($R = 0.3$ m, $a = 0.1$ m). Measurements presented in this paper were done in discharges with $B = (1\text{–}1.4)$ T, $\bar{n}_e = (0.5\text{–}3) \times 10^{19}$ m^{-3} and $I_p \approx (30\text{–}40)$ kA.

A square array of four Langmuir probes was used to characterize edge fluctuations. Two tips, aligned perpendicular to the toroidal magnetic field, are used to measure the poloidal phase velocity of the fluctuations. The poloidal phase velocity of the fluctuations reverses propagation (velocity shear layer) from the ion to the electron drift direction in the proximity of the limiter radius. Radial electric fields were externally applied by means of a biased electrode.

Density and electron temperature profiles were obtained from Thomson scattering measurements. Temperature pulses induced by sawteeth were deduced from soft X ray tomography; density pulses were monitored by a microwave interferometer and by a two-channel reflectometer. Radiation profiles were measured by a bolometer array.

Proton and impurity temperatures have been deduced from Doppler line broadening of hydrogen (line wings) and impurity lines (CV 2271 Å).

3. THE EFFECT OF ATOMIC PHYSICS MECHANISMS AND RADIAL ELECTRIC FIELDS ON EDGE TURBULENCE

Probe current ($\tilde{I}_s/I_s$), temperature ($\tilde{T}_e/T_e$) and density ($\tilde{n}/n$) fluctuations have been determined by sweeping the applied voltage (V) to a single Langmuir probe at a frequency of 300 kHz [1]. The current–voltage characteristic has been fitted by the expression

$$I = I_s(1 - \exp[e(V - V_f)/kT_e])$$

where I_s is the ion saturation current and V_f is the floating potential. The ion saturation current is linearly proportional to the local plasma density (n) and to the velocity (v) of the ions entering the probe sheath. The velocity is taken as

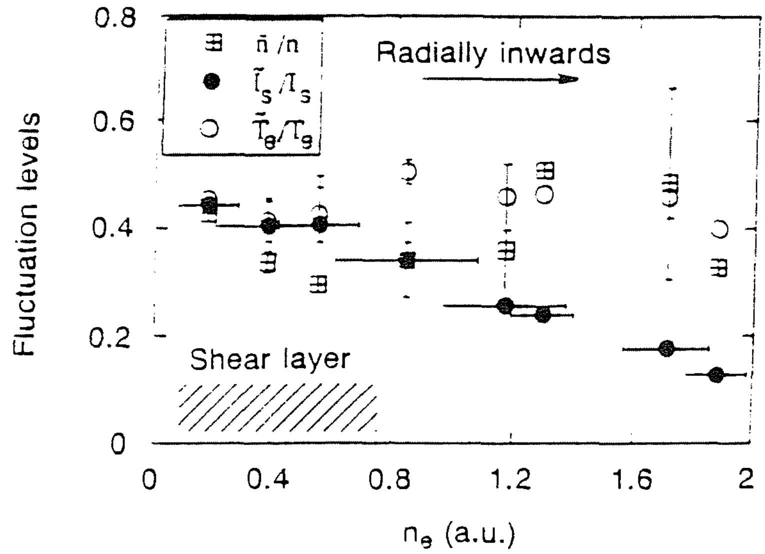

FIG. 1. Temperature, current and density fluctuations versus local electron density close to the limiter radius.

$v \propto (T_e/m_i)^{1/2}$. Using a non-linear least square fitting routine, we have determined the electron temperature, the ion saturation current and deduced the local plasma density ($n \propto I_s T_e^{-1/2}$) in a time-scale of about 2 μs.

Fluctuations in the ion saturation current decrease when the probe moves radially inwards (Fig. 1). However, whereas $\tilde{I}_s/I_s$, $\tilde{T}_e/T_e$ and $\tilde{n}/n$ are comparable near the shear layer location, $\tilde{I}_s/I_s$ is smaller than both $\tilde{n}/n$ and $\tilde{T}_e/T_e$ in the plasma edge region ($r/a_{shear} < 1$). If we take into account that the ion saturation current is proportional to the local electron density and to the square root of the electron temperature, the present results imply that there are significant edge temperature fluctuations which are in phase close to opposition with the corresponding density fluctuations. Ionization processes, acting simultaneously as an electron energy sink and electron density drive, might provide a coupling in phase opposition between density and temperature fluctuations. Alternatively, if the pressure balance condition is fulfilled [2], a phase opposition between density and temperature fluctuations is expected.

The experimental signature of radiative instabilities is the presence of substantial temperature fluctuations. In the case of the condensation drive, significant coupling between density and temperature fluctuations is expected. The fulfilment of these general requirements in the present experiment makes condensation drive an attractive candidate partially explaining edge turbulence features. However, other models would also predict significant temperature fluctuations. More systematic studies of the correlation between radiation and turbulence levels are needed to fully clarify the role of radiation in edge turbulence.

Two different approaches have been used to study the effect of radial electric fields on edge turbulence. First, the influence of the naturally induced radial electric

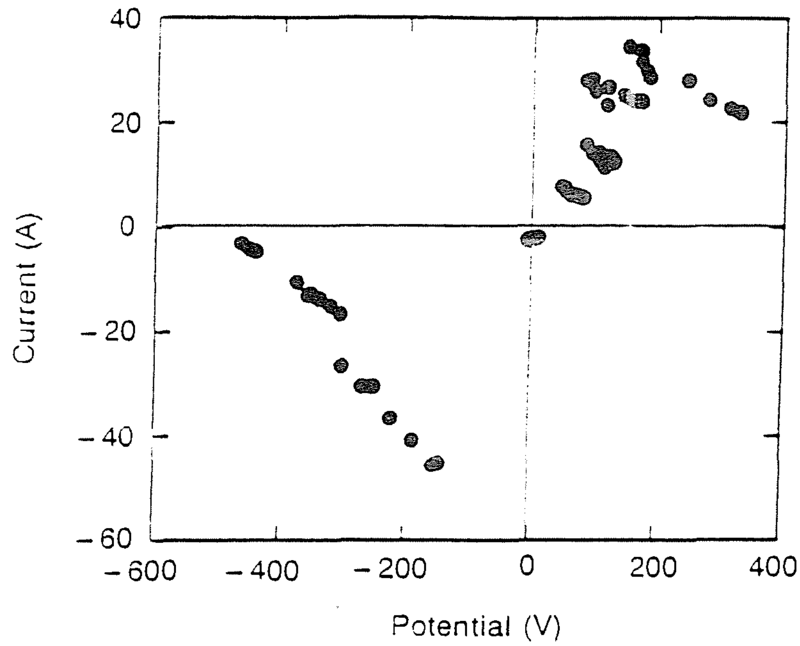

FIG. 2. Current-voltage electrode characteristic (B = 1 T, $I_p \approx 40$ kA).

fields on edge electrostatic and magnetic fluctuations has been studied. Second, the effect of biased electrodes on turbulence and confinement is under investigation.

Plasma profiles, fluctuation levels ($\tilde{I}_s/I_s$), the coherence between probes which measure the floating potential and are poloidally separated by 0.3 cm are modified near the velocity shear layer location. The autocorrelation time remains basically constant when moving through the shear layer region. Furthermore, the shear strength (dv/dr) appears to be sensitive to the plasma conditions. However, no direct correlation between sheared poloidal flows and turbulence characteristics has been observed, so far.

Positive and negative biased electrodes (± 1000 V) have been applied in the edge region of TJ-I. The current-voltage characteristic of the electrode shows a reduction in the current as the bias increases to values higher than 200 V for both polarities (Fig. 2). Preliminary results show a modification in the global plasma behaviour when biasing is applied to the electrode. High frequency fluctuations (≈ 300 kHz) with low poloidal wavenumber and, possibly, of magnetic nature have been observed in the Langmuir probe current monitor when positive biasing is applied to the electrode.

4. TRANSPORT STUDIES BY STEADY STATE AND PERTURBATIVE METHODS

In a general formulation, the dependence of particle (Γ) and electron energy fluxes (q) on density and temperature gradients may be written as:

$$\Gamma = -D\nabla n - D_T \frac{n}{T} \nabla T - W_n F + \sum_{i,j,k} D_{ijk}(\nabla n)^i (\nabla T)^j F^k$$

$$q = Q - \frac{5}{2} \Gamma T = -\chi_n T \nabla n - \chi n \nabla T - W_T F + \sum_{i,j,k} \chi_{ijk}(\nabla n)^i (\nabla T)^j F^k$$

where F is any other force as, e.g. the parallel or the radial electric field.

A perturbative experiment, such as the simultaneous measurement of density and temperature pulses induced by a sawtooth collapse, give us the derivatives of the fluxes with respect to the gradients. By following the method of coupled analysis presented in Ref. [3], density and temperature pulses are combinations of fast and slow eigenmodes. From the experimental measurements the matrix A that governs pulse propagation can be obtained:

$$\frac{\partial}{\partial t}\begin{pmatrix}\tilde{n}/n \\ \tilde{T}/T\end{pmatrix} = -A\nabla^2 \begin{pmatrix}\tilde{n}/n \\ \tilde{T}/T\end{pmatrix}, \qquad A_{11} = -\frac{\partial \Gamma}{\partial \nabla n} \qquad A_{12} = -\frac{T}{n}\frac{\partial \Gamma}{\partial \nabla T}$$

$$A_{21} = \frac{2}{3}\left(A_{11} - \frac{1}{T}\frac{\partial q}{\partial \nabla n}\right) \qquad A_{22} = \frac{2}{3}\left(A_{12} - \frac{1}{n}\frac{\partial q}{\partial \nabla T}\right)$$

Figure 3 shows temperature and density pulses induced by sawteeth at $r/a \approx 0.4$ in the TJ-I tokamak. The temperature pulse is dominated by the fast eigenmode and the density pulse by the slow one plus pulse overlapping. The matrix A for this case is:

$A_{11} = 1.2 \pm 0.1\ m^2/s \qquad A_{12} = 0.0 \pm 0.3\ m^2/s$

$A_{21} = 0.8 \pm 0.3\ m^2/s \qquad A_{22} = 5.9 \pm 0.1\ m^2/s$

Matrix coefficients scale with the inverse of local density and the square of magnetic field, $A_{ij} = A_{ij0}/nB^2$. It must be noted that this scaling could also be a scaling in safety factor and Z_{eff}.

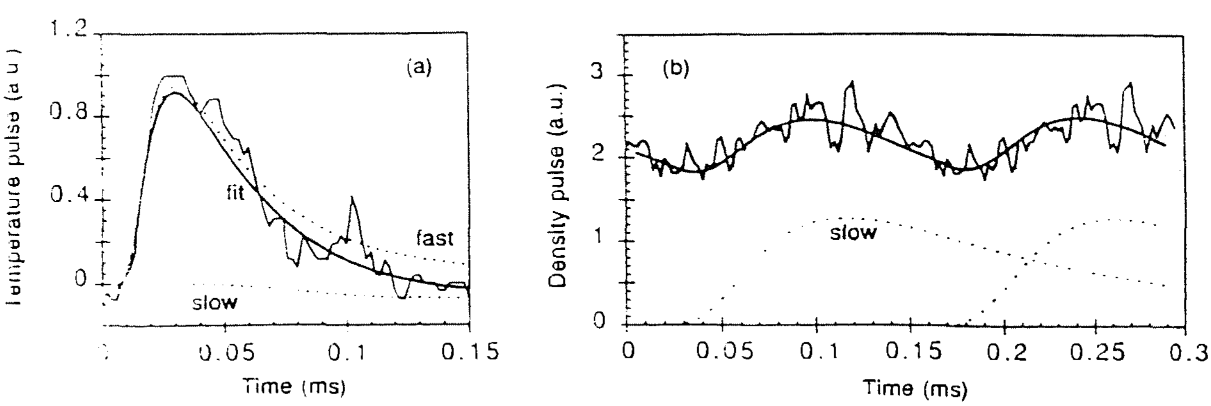

FIG. 3. Time evolution of temperature (a) and density (b) pulses and the two eigenmode fittings at $r/a \approx 0.4$.

If the transport is dominated by first order terms we can obtain the transport coefficients from the matrix A, except for those related to forces F or pinches. To test this linear assumption and the significance of the forces F, we have compared the electron energy flux obtained from steady state analysis with the predicted flux using the coefficients obtained from sawtooth analysis, $Q = -1.2 \times (2 \times 10^{19}/n) \times (2.5\, T\nabla n + 7.4\, n\nabla T)$. The agreement is good enough to imply that non-linearities are not important and that the heat pinch does not seem to be needed at $r/a \approx 0.4$. The agreement also means that χ obtained from sawtooth coupled analysis and from steady state transport analysis has the same value.

Assuming that the value for the ratio $\chi/D \approx 7$, found in the sawtooth pulse propagation experiment, is valid for different plasma radii, we can determine, from steady state analysis, the radial profiles of χ and D, together with the particle pinch. The pinch obtained is very close to a neoclassical pinch in the plasma core ($r/a < 0.6$).

The results obtained in this work allow us to describe the transport in the plasma core in a simple way, valid at the same time for steady state and sawtooth pulse propagation conditions. In this description the particle flux is independent of the temperature gradient and has a pinch very close to the neoclassical Ware pinch. Nevertheless, the diffusion coefficient is an order of magnitude higher than the neoclassical one. The conductive electron heat flux depends only on the temperature gradient with a heat conductivity seven times greater than the diffusion coefficient. The high value of χ/D suggests a transport mechanism dominated by the fast electrons. The collisional regime cancels any effect of trapped particles and the low beta forbids the use of any standard model of magnetic turbulence. Enhanced transport due to an ergodic magnetic field by island overlapping and error fields could be a plausible explanation.

5. THE EFFECT OF NON-THERMAL FLUCTUATING VELOCITIES IN ANOMALOUS IMPURITY HEATING

Proton and impurity temperature profiles have been measured from spectral line widths in the TJ-I tokamak. Impurity ions exhibit higher temperature than protons, the difference being a decreasing function of electron density [4]. Anomalous heating of impurities or both proton and impurities has been reported in several devices (Ref. [5] and references therein).

The observed impurity temperatures in TJ-I can be understood by considering the influence of non-thermal velocity fluctuations on the spectral line widths. The influence of plasma turbulence on spectral line widths has been included by a method used in astrophysics [6]. If the spectral line shape is the result of the convolution of a thermal Gaussian and a turbulent Gaussian distribution, the latter producing a gross mass motion, the full width at half maximum of the resulting line is given by

$$\Delta\lambda = 1.665\ (\lambda/c)\ [(2kT_i/m_i) + \xi^2]^{1/2}$$

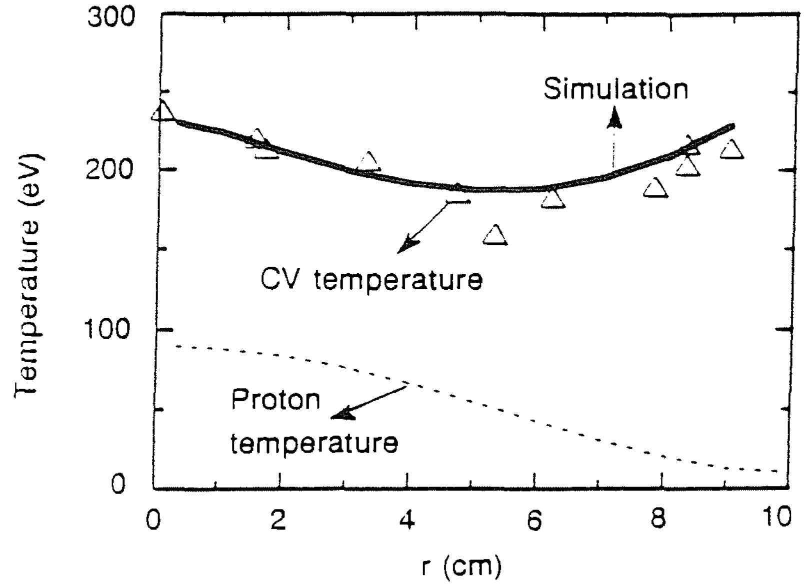

FIG. 4. Comparison of CV (open triangles) and proton (dashed curved) temperature profiles in a low density discharge ($\bar{n}_e \approx 1 \times 10^{13}$ cm^{-3}). The simulated curve was obtained by including the effect of fluctuating radial and poloidal electric fields.

where ξ is the dispersion of the Gaussian microturbulence velocity distribution and λ is the spectral line wavelength. If the non-thermal velocities do not depend on the charge and mass of the particle, their influence on the line widths of protons and impurity ions with long ionization times will be different and can be identified unambiguously.

For a typical low density discharge, in Fig. 4 we show the temperature profiles of the CV ions (chord integrated) and protons. The continuous curve represents the result of simulating the impurity temperature profile when non-thermal velocity fluctuations with appropriate radial dependence are present in the plasma. Assuming that the non-thermal velocity fluctuations are due to $\vec{E} \times \vec{B}$ drifts, the equivalent radial (E_r [V/cm]) and poloidal (E_θ [V/cm]) fluctuating electric fields needed to account for this effect are given by

$$\langle E_r \rangle_{rms} = 400 \times \exp[-(10 - r)/8] \qquad \langle E_\theta \rangle_{rms} = 500 \times \exp[-r/10]$$

The deduced root mean square values of the radial fluctuating electric fields are consistent with probe measurements in tokamaks [7]; the measured values of E_r in the edge region of TEXTOR are of the order of 150 V/cm which are comparable to the values deduced in the present work ($\approx$200 V/cm) at $\bar{n}_e \approx 2.5 \times 10^{19}$ m^{-3}. In contrast, the values deduced for the poloidal fluctuating electric fields are much higher than those estimated by Langmuir probes in the edge region of the TJ-I tokamak ($\approx$20 V/cm).

Since TJ-I plasma parameters are similar to those prevailing at the edge of large devices, this work has two consequences for the periphery of fusion relevant plasmas.

First, the high edge ion temperature reported from other tokamaks could be due to a similar mechanism. Second, if measurements of proton and impurity temperatures are available, information about fluctuating electric field levels might be obtained.

6. CONCLUSIONS

Studies of edge turbulence and transport have been performed in the TJ-I tokamak. The results can be summarized as follows:

(i) Evidence of substantial temperature fluctuations has been found in the plasma edge region. Furthermore, $\tilde{T}_e/T_e$ and $\tilde{n}/n$ are fluctuating in phase close to opposition. Radiative instabilities, and in particular the condensation effects, could play a key role in driving plasma edge fluctuations.

(ii) Evidence of electrostatic turbulence characteristics modified in the proximity of the velocity shear layer has been obtained. Radial electric fields externally applied in the plasma edge induce changes in the edge and global plasma parameters.

(iii) In the plasma core region, the coefficients that govern the particle and electron heat transport are the same for both steady state and pulse propagation experiments. The particle pinch is close to the neoclassical pinch, and there is no evidence of a significant heat pinch.

(iv) Measurements of proton and impurity temperature profiles from spectral line widths reveal that, in addition to thermal line broadening, the influence of non-thermal velocity fluctuations due to stochastic fields should be considered in order to account for the observed impurity temperatures.

ACKNOWLEDGEMENTS

This work was partially supported by the Dirección General de Investigaciones Científicas y Técnicas of Spain under project numbers PB90-0639 and PB90-0410.

REFERENCES

[1] BALBÍN, R., HIDALGO, C., PEDROSA, M.A., GARCÍA-CORTÉS, I., VEGA, J., Rev. Sci. Instrum. (1992) (in press).

[2] THRAYER, D.R., DIAMOND, P.H., Phys. Fluids **30** (1987) 3724.

[3] De HAAS, J.C.M., O'ROURKE, J., SIPS, A.C.C., LOPES CARDOZO, N.J., Nucl. Fusion **31** (1991) 1261.

[4] ZURRO, Z., HIDALGO, C., GARCÍA-CASTAÑER, B., PARDO, C., Plasma Phys. Control. Fusion **32** (1990) 565.

[5] McCHESNEY, J.M., BELLAN, P.M., STERN, R.A., Phys. Fluids B **3** (1991) 3363.

[6] GRAY, D.F., Lectures on Spectral Line Analysis: F, G, and K Stars., Aylmer Express Ltd, Aylmer, Ontario (Canada) 1988.

[7] BORA, D., IVANOV, R.S., VAN OOST, G., SAMM, U., Nucl. Fusion **31** (1991) 2383.

DISCUSSION

H.Y.W. TSUI: I observe that the normalized electron temperature fluctuation level in the edge plasma of TJ-1 is about twice that of TEXT. The curve fitting technique requires a short time interval to measure the electron temperature. Do you think that movement of the turbulent structure during this time interval would have any effect on the measurement of the electron temperature fluctuation?

C. HIDALGO: Variations in the structure of the turbulence during the sweeping time of the probe contribute to the total uncertainty associated with the electron temperature fluctuations deduced from the fast swept Langmuir probe method. Using a sweeping frequency of 300 kHz and taking into account the fact that fluctuations are dominated by frequencies below 100 kHz in the edge region of TJ-1, we should find that such uncertainties produce 'apparent' temperature fluctuations of about 10% in the present experiment.

R.J. GOLDSTON: The traditional approach to estimating the effect of turbulent velocities on the Doppler temperature of impurities in tokamaks has been to assume that the turbulent velocity field non-linearly saturates with $v \sim v_{dia}$. Does this sort of model roughly match your data?

C. HIDALGO: We have, so far, only compared the root mean square values of the deduced fluctuating electric fields with the measured values in the edge region of different tokamaks.

P.M. BELLAN: A few years ago at Caltech we found[1] a stochastic ion heating mechanism which may explain your anomalous ion heating. This mechanism — which was observed experimentally and satisfactorily modelled — causes ion heating if $(m_i k^2 \phi_{rms}/q_i B^2) > 0.3$. It might be worth while seeing whether your parameters satisfy this threshold condition.

[1] McCHESNEY, J.M., STERN, R.A., BELLAN, P.M., Phys. Rev. Lett. **59** (1987) 1436; McCHESNEY, J.M., BELLAN, P.M., STERN, R.A., Phys. Fluids B 3 (1991) 3363.

PHYSICS STUDIES FOR THE TORSATRON TJ-IU

C. ALEJALDRE, E. ASCASIBAR, F. CASTEJON, L. GARCIA, J. GUASP,
A. LOPEZ-FRAGUAS, A. PEREZ-NAVARRO, A. RODRIGUEZ-YUNTA,
A. SALAS, A. VARIAS
Asociación Euratom–CIEMAT para fusión,
Madrid, Spain

Abstract

PHYSICS STUDIES FOR THE TORSATRON TJ-IU.

TJ-I Upgrade (TJ-IU) is a six period, $\ell = 1$ torsatron in the final stages of construction at CIEMAT, Madrid. Its major radius is 0.6 m and its average plasma radius 0.1 m. The device was designed to bridge the gap between the TJ-I tokamak actually working at CIEMAT and the Heliac TJ-II that will start operation in 1995. TJ-IU will share with TJ-I its power supplies and peripherals — hence its name. The main theoretical predictions as to equilibrium, stability, transport and kinetic theory are described.

1. DESCRIPTION OF THE DEVICE

The required magnetic field of TJ-I Upgrade (TJ-IU) is created by the five coil system shown in Fig. 1. The main helical coil winding follows the law:

$$\phi = (1/6)\ (\theta + 0.4 \sin\theta)$$

where ϕ is the toroidal and θ the poloidal angle. This modulation is essential to achieving a deep magnetic well with moderate ripple at axis. The helical coil has 20 turns, with a total current of 280 kA turn. In addition to the helical coil, two pairs of vertical field coils are needed. The external pair has a radius of 1 m and is placed at 0.35 m of height, symmetrically up and down the equatorial plane; the internal pair has a radius of 0.30 m and a height of 0.40 m. For the standard case the external pair current is 122 kA turn, opposite to the helical current, while the internal pair current is 49 kA turn. Two pairs of additional coils are also used in order to compensate small currents in the plasma.

The device has been designed to have a wide operational flexibility, i.e. different values of rotational transform and magnetic well depth can be achieved by changing the ratio between the currents of the vertical field and the helical coils. This change shifts the magnetic axis of the position, thereby producing the basic configuration variation. With due account for the current limits imposed by the available power supplies, TJ-IU can shift its magnetic axis between 6 cm inside and 3 cm outside the nominal R_0 (R_0 = 0.58 m). This shift produces a range for the rotational transform at axis of $0.14 \leq \iota(0) \leq 0.40$ while the shear may be changed between -5% and 37% and the magnetic well depth between 0% and 7%, always maintaining

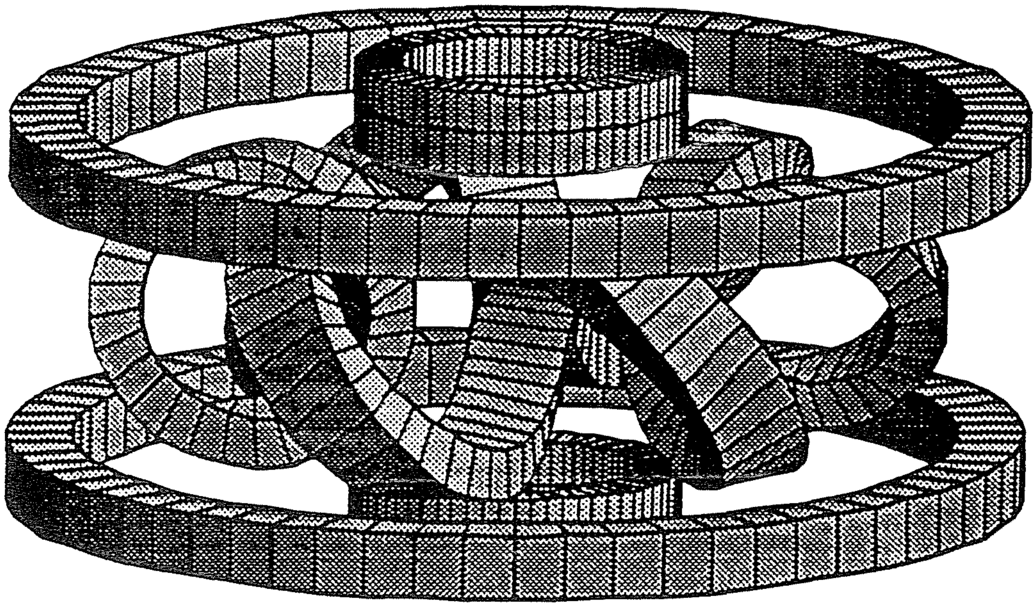

FIG. 1. TJ-IU coil configuration.

an average plasma radius greater than 7 cm and the magnetic field intensity of 0.52 T at the magnetic axis with a magnetic ripple of 7.6%. Startup and heating will be done initially with a 200 kW, 28 GHz gyrotron working at the second harmonic; an ion cyclotron heating (ICH) system is under design. Magnetic surface mapping experiments are expected to begin in November 1992 and first plasmas by spring 1993.

2. EQUILIBRIUM AND STABILITY

The strong modulation of the helical coil produces a deep vacuum magnetic well (7%). This is the main stability mechanism in the machine since its shear is almost negligible for the configuration with the magnetic axis at its 'standard' position (0.58 m). The average radius of the last closed magnetic surface inside the vacuum chamber is $\langle a \rangle \approx 10$ cm. The average toroidal field at axis is 0.62 T, with a magnetic ripple of 7.6%.

With the fixed boundary version of the 3-D code VMEC [1], equilibria for two different configurations of the machine have been obtained, and a sequence of zero net current equilibria has been generated. Figure 2 shows the equilibrium magnetic axis shift for the standard configuration, and Fig. 3 shows the flux surfaces at four toroidal positions for this case $\langle \beta \rangle \approx 2\%$. The Shafranov shift of the surfaces and the helicity of the magnetic axis are to be seen clearly. The position at $\zeta = 30°$, corresponding to the most triangular cross-section, is the one chosen for microwave injection. The pressure profile used is the usual $p \propto (1 - \Phi)^2$, where Φ is the toroidal flux normalized to 1 at the edge. The two configurations considered are the 'standard' one for which parameters such as plasma volume, magnetic well depth, etc.

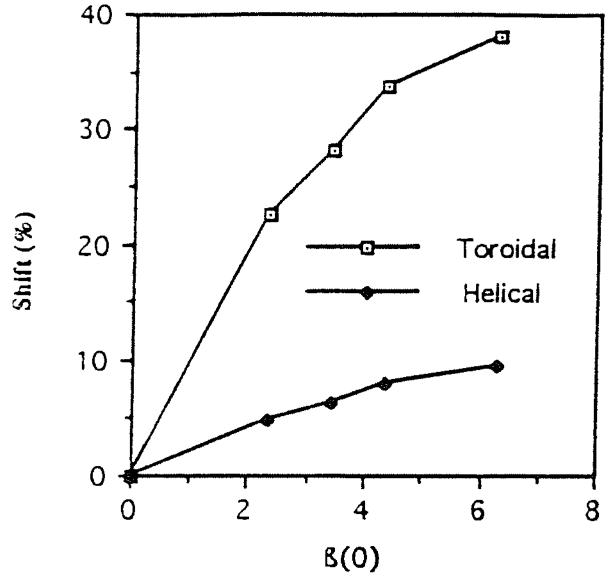

FIG. 2. Toroidal and helical shifts for increasing pressure.

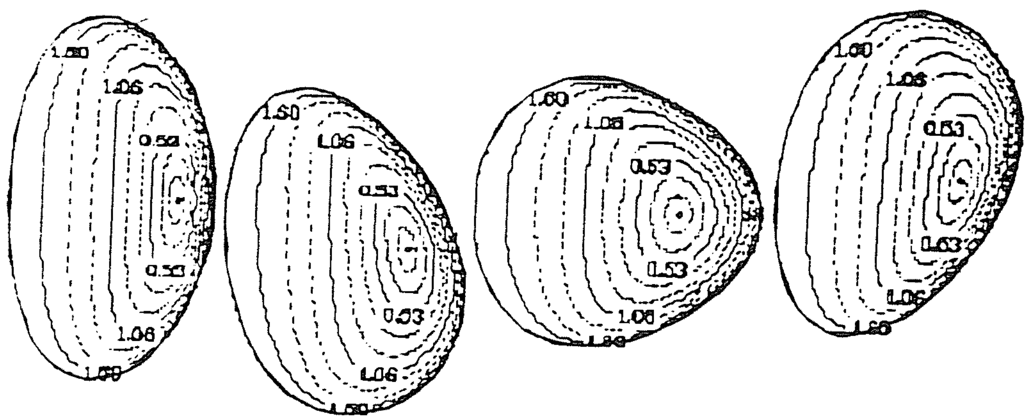

FIG. 3. Flux surfaces of the standard configuration at ⟨β⟩ ≈ 2% for four toroidal positions (ζ = 0°, 15°, 30° and 45°).

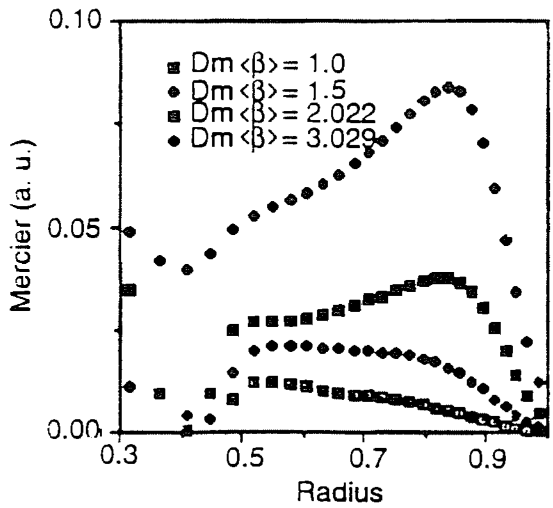

FIG. 4. Mercier criterion (D_M) in arbitrary units for several values of the pressure versus radius.

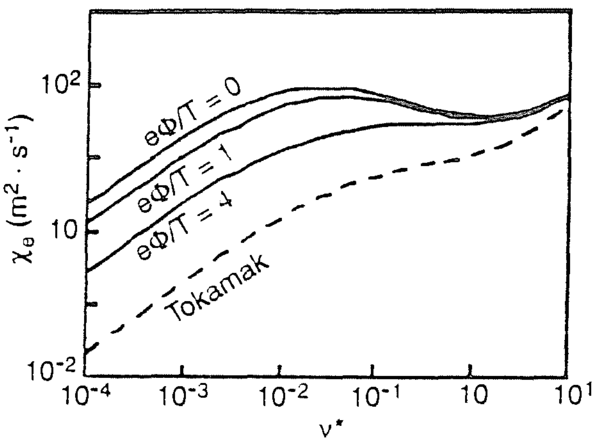

FIG. 5. χ_e versus collisionality and radial electric field in TJ-IU.

have been optimized and the 'inward' configuration, characterized for a position of the magnetic axis in vacuum shifted 6 cm towards the axis of the machine. The equilibrium quantities obtained have then been used to evaluate the 3-D Mercier stability criterion for local instabilities [2]. Figure 4 summarizes the results obtained for the standard configuration. A positive D_M satisfies the stability criterion for Mercier modes. The configuration is stable to Mercier modes for the whole radius and pressures considered, even at $\langle\beta\rangle = 3\%$. The valley in the criterion at average radius 0.4 is due to the passing through a lower order resonance of the iota profile that should flatten the pressure profile. We have chosen Mercier modes for our β studies since they have been shown to give a limit to the pressure in other torsatrons [3]. Nevertheless, a study is under way to check the TJ-IU stability to ballooning modes. From the Mercier studies we can conclude that the β limit in TJ-IU is well above the achievable β value for the 200 kW of ECH heating power available initially although the possibility to inject 600 kW of ICH in a second phase will permit us to reach β values closer to its theoretical limit in some configurations.

This stability picture changes dramatically when we push the magnetic axis inwards, towards the centre of the machine. The stabilizing vacuum magnetic well is destroyed and the configuration becomes unstable to Mercier modes, even at very low values of the pressure. This strong stability antagonism between both configurations will permit us to experimentally check the influence, if any, of the fraction of trapped particles on the stability of the machine. This fraction changes considerably from 11% for the standard configuration to 68% for the inward one.

3. TRANSPORT

Calculations of neoclassical transport coefficients for the TJ-IU have been made by means of a Monte Carlo code [4, 5]. Figure 5 shows the neoclassical electron heat conductivity versus collisionality for several values of the radial electric field. The

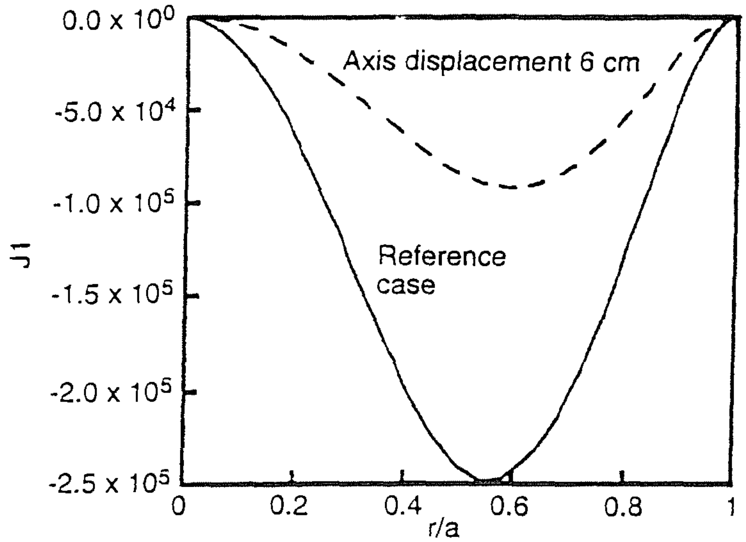

FIG. 6. Bootstrap current density in TJ-IU.

axisymmetric coefficient for equal rotational transform is also shown for comparison as a dashed line. Evidently, the neoclassical transport in TJ-IU is higher than in the equivalent tokamak for all regimes including the plateau and collisional regime. Displacing the magnetic axis inwards we can change the magnetic field configuration and obtain a lower effective field ripple, improving the transport properties by a factor of two. It is worth while to note that transport and stability seem to improve in opposite direction with respect to magnetic axis shift.

By assuming parabolic profiles for density, temperature and radial electric potential, a simple estimate of the neoclassical confinement times on the half-radius surface was found. The magnitude of the electric field was taken from the solution of the ambipolarity condition, $\Gamma_e(\Phi') = \Gamma_i(\Phi')$. Taking as central temperatures for an electron cyclotron heating (ECH) scenario, $T_e(0) = 400$ eV, $T_i(0) = 50$ eV and a density of $n_e(0) = 0.5 \times 10^{13}$ cm^{-3}, the ambipolar electric potential was found to be $e\Phi = 350$ eV, the particle confinement time $\tau_p = 0.37$ ms and the energy confinement time $\tau_E = 0.17$ ms in the reference case. In the case of a displaced magnetic axis (6 cm) the results were $e\Phi = 100$ eV, $\tau_p = 0.50$ ms and $\tau_E = 0.25$ ms.

Calculations of bootstrap currents in TJ-IU have been also made by means of the analytical expressions for non-axisymmetric devices of Ref. [6, 7]. Figure 6 shows the expected current profiles for the reference case and for the case with inwards displacement of the magnetic axis. The total currents are 3.7 kA and 1.6 kA, respectively, with their direction opposite to the magnetic field. As in radial transport, the magnitude is lower for the displaced axis case.

4. ELECTRON CYCLOTRON CURRENT DRIVE

One of the main topics of research on this machine will be the study of ECH plasmas and, in particular, of the possibility to compensate induced currents such as bootstrap and rotational transform effects by using electron cyclotron (EC) waves. The induced current, parallel to the magnetic field, in the TJ-IU torsatron was computed in terms of the relativistic response function and the absorbed power density [8]:

$$J_{\parallel}(\vec{r}) = -\frac{mc^2}{8\pi n\Lambda e^3}\int d\vec{v}\,\eta(\vec{v})\sum_s w_s(\vec{v})$$

where n, m and e are the electron density, mass and charge, respectively, c is the speed of light, Λ is the Coulomb logarithm and $\vec{v} = \vec{p}/mc$.

For arbitrary diffusion in momentum space, i.e. for any kind of wave, the microscopic efficiency can be written as [9]:

$$\eta(\vec{v}) = \frac{\delta J_{\parallel}}{\delta P_d} = G(v)\left[N_{\parallel} - \frac{v_{\parallel}}{v^2}(\gamma + 1 + Z)\right] + \frac{2vv_{\parallel}}{\gamma^2}$$

where we have introduced the function

$$G(v) = \frac{2}{v}\left[\frac{\gamma(v)+1}{\gamma(v)-1}\right]^{\frac{1+Z}{2}}\int_0^v dx\left[\frac{x}{\gamma(x)}\right]^3\left[\frac{\gamma(x)-1}{\gamma(x)+1}\right]^{\frac{1+Z}{2}}$$

and $\gamma(x) = (1 + x^2)^{1/2}$.

The absorbed power density in phase space is calculated for EC waves at a harmonic of order s, for a Maxwellian distribution function and at first order in the Larmor radius. We introduce a macroscopic current drive efficiency in the plasma:

$$\gamma(\vec{r}) = -\frac{mc^2}{8\pi n\,\Lambda e^3}\,\frac{\int d\vec{v}\,\eta(\vec{v})\sum_s w_s(\vec{v})}{\int d\vec{v}\sum_s w_s(\vec{v})}$$

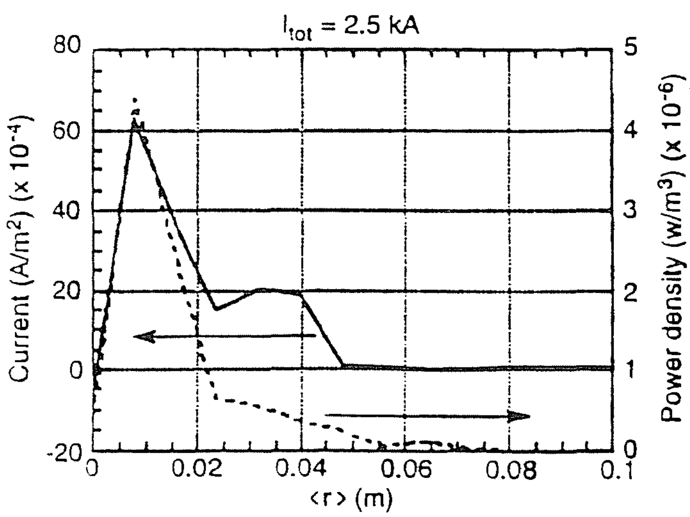

FIG. 7. Absorbed power and induced current density versus radius obtained with one 200 kW, 28 GHz gyrotron launched in the X-mode ($n_e = 0.5 \times 10^{19}\ m^{-3}$ and $T_e = 0.5$ keV).

and the induced current density will be

$$J_i(\vec{r}) = \gamma(\vec{r})W_s(\vec{r})$$

The mean absorbed power density at a magnetic surface is calculated by using the ray tracing code RAYS [10] and the volume of the magnetic surface considered is computed in terms of magnetic co-ordinates. The plasma parameters needed to calculate the efficiency are also given by the code.

The microwave beam is considered to be 5 cm wide which is not negligible because the plasma minor radius is about 10 cm. To take this fact into account we simulate the microwave beam by a set of 64 rays weighted by a Gaussian. So the actual current density will be given by

$$J(\langle r\rangle) = \frac{1}{\sum_{i = \text{rays}} \exp(-x_i^2/(d/2)^2)} \sum_{i = \text{rays}} J_i(\langle r\rangle) \exp(-x_i^2/(d/2)^2)$$

The results for a typical case are shown in Fig. 7, where the absorbed power and the induced current densities are plotted against the mean minor radius. The launched power is 200 kW at the second harmonic (f = 28 GHz) of the X-mode. Even though the plasma density and temperature are not very high ($n = 0.5 \times 10^{19}\ m^{-3}$ and $T = 0.5$ keV) we obtain a rather high current of 2.5 kA because the volume of the device is small and therefore we usually have a high power density. The total current is obtained by integrating the current density, which is a function of the particular magnetic surface:

$$I = \int \vec{J}\cdot d\vec{S} = 2\pi \int_0^a \langle r\rangle\, J(\langle r\rangle)\, d\langle r\rangle$$

5. CONCLUSIONS

The standard configuration of TJ-IU is stable to ideal interchange modes for values of β much higher than those achievable with the available power. Trapped particle effects could be visible experimentally.

Neoclassical transport and bootstrap current are very sensitive to the shift of the magnetic axis in TJ-IU. This feature will allow experimental testing of theoretical models.

TJ-IU high power density value enables the attaining of relatively high EC driven currents that will make possible the compensation of plasma currents induced by bootstrap or iota effects.

REFERENCES

[1] HIRSHMAN, S.P., VAN RIJ, W.I., MERKEL, P., Comput. Phys. Commun. **43** (1986) 143.

[2] BAUER, F., BETANCOURT, O., GARABEDIAN, P., WAKATANI, M., The BETA Equilibrium, Stability and Transport Code, Springer Verlag, New York (1987).

[3] CARRERAS, B.A., DOMINGUEZ, N., GARCIA, L., LYNCH, V.E., LYON, J.F., CARY, J.D., NAVARRO, A.P., Nucl. Fusion **28** (1988) 1195.

[4] FOWLER, R.H., ROME, J.A., LYON, J.F., Phys. Fluids **28** (1981) 851.

[5] LOTZ, W., NÜHRENBERG, J., SCHLÜTER, A., J. Comput. Phys. **73** (1987) 73.

[6] SOLANO, E.R., SHAING, K.C., Phys. Fluids **30** (1987) 462.

[7] SHAING, K.C., et al., Phys. Fluids B **1** (1989) 1663.

[8] CASTEJÓN, F., ALEJALDRE, C., COARASA, J.A., Current driver by electron cyclotron waves in stellarators, Phys. Fluids B **1** (1992) 1761.

[9] FISCH, N.J., Phys. Rev. A **24** (1980) 3245.

[10] ALEJALDRE, C., CASTEJÓN, F., TABOADA, M.J., in Controlled Fusion and Plasma Physics (Proc. 16th Eur. Conf. Venice, 1989), Vol. 13B, Part III, Eureopean Physical Society (1989) 1115.

CIEMAT - 723
Centro de Investigaciones Energéticas, Medioambientales y Tecnológicas
Instituto de Investigación Básica.- Madrid

Papers presented at the FOURTEENTH INTERNATIONAL CONFERENCE ON PLASMA PHYSICS AND CONTROLLED NUCLEAR FUSION RESEARCH
Organización Internacional de la Energía Atómica
Würzburg, Alemania
30 Septiembre - 7 Octubre 1992

34 pp., 17 figs., 25 refs.

This report contains the contributions of the CIEMAT's Fusion Unit to the 14th International Conference on Plasma Physics and Controlled Nuclear Fusion Research that was held by the International Atomic Energy Agency in Würzburg, Germany from 30 September to 7 October 1992. Three papers were presented that summarized the main lines of work done in the Unit during the previous two years: The first one on the theoretical advances in the understanding of the Fexible Heliac TJ-II under construction, the second on the confinement studies performed in the operating TJ-I Tokamak and the third one on the description of the physical properties of the soon to be started TJ-IU Torsatron.

DOE CLASIFICATION AND DESCRIPTORS: 700310, PLASMA CONFINEMENT, THERMONUCLEAR DEVICES, HELIAC STELLARATORS, TROSATRON STELLARATORS, TOKAMAK DEVICES, THERMONUCLEAR REACTIONS, THERMONUCLEAR REACTORS

CIEMAT - 723
Centro de Investigaciones Energéticas, Medioambientales y Tecnológicas
Instituto de Investigación Básica.- Madrid

Papers presented at the FOURTEENTH INTERNATIONAL CONFERENCE ON PLASMA PHYSICS AND CONTROLLED NUCLEAR FUSION RESEARCH
Organización Internacional de la Energía Atómica
Würzburg, Alemania
30 Septiembre - 7 Octubre 1992

34 pp., 17 figs., 25 refs.

This report contains the contributions of the CIEMAT's Fusion Unit to the 14th International Conference on Plasma Physics and Controlled Nuclear Fusion Research that was held by the International Atomic Energy Agency in Würzburg, Germany from 30 September to 7 October 1992. Three papers were presented that summarized the main lines of work done in the Unit during the previous two years: The first one on the theoretical advances in the understanding of the Fexible Heliac TJ-II under construction, the second on the confinement studies performed in the operating TJ-I Tokamak and the third one on the description of the physical properties of the soon to be started TJ-IU Torsatron.

DOE CLASIFICATION AND DESCRIPTORS: 700310, PLASMA CONFINEMENT, THERMONUCLEAR DEVICES, HELIAC STELLARATORS, TROSATRON STELLARATORS, TOKAMAK DEVICES, THERMONUCLEAR REACTIONS, THERMONUCLEAR REACTORS

CIEMAT - 723
Centro de Investigaciones Energéticas, Medioambientales y Tecnológicas
Instituto de Investigación Básica.- Madrid

Papers presented at the FOURTEENTH INTERNATIONAL CONFERENCE ON PLASMA PHYSICS AND CONTROLLED NUCLEAR FUSION RESEARCH
Organización Internacional de la Energía Atómica
Würzburg, Alemania
30 Septiembre - 7 Octubre 1992

34 pp., 17 figs., 25 refs.

This report contains the contributions of the CIEMAT's Fusion Unit to the 14th International Conference on Plasma Physics and Controlled Nuclear Fusion Research that was held by the International Atomic Energy Agency in Würzburg, Germany from 30 September to 7 October 1992. Three papers were presented that summarized the main lines of work done in the Unit during the previous two years: The first one on the theoretical advances in the understanding of the Fexible Heliac TJ-II under construction, the second on the confinement studies performed in the operating TJ-I Tokamak and the third one on the description of the physical properties of the soon to be started TJ-IU Torsatron.

DOE CLASIFICATION AND DESCRIPTORS: 700310, PLASMA CONFINEMENT, THERMONUCLEAR DEVICES, HELIAC STELLARATORS, TROSATRON STELLARATORS, TOKAMAK DEVICES, THERMONUCLEAR REACTIONS, THERMONUCLEAR REACTORS

CIEMAT - 723
Centro de Investigaciones Energéticas, Medioambientales y Tecnológicas
Instituto de Investigación Básica.- Madrid

Papers presented at the FOURTEENTH INTERNATIONAL CONFERENCE ON PLASMA PHYSICS AND CONTROLLED NUCLEAR FUSION RESEARCH
Organización Internacional de la Energía Atómica
Würzburg, Alemania
30 Septiembre - 7 Octubre 1992

34 pp., 17 figs., 25 refs.

This report contains the contributions of the CIEMAT's Fusion Unit to the 14th International Conference on Plasma Physics and Controlled Nuclear Fusion Research that was held by the International Atomic Energy Agency in Würzburg, Germany from 30 September to 7 October 1992. Three papers were presented that summarized the main lines of work done in the Unit during the previous two years: The first one on the theoretical advances in the understanding of the Fexible Heliac TJ-II under construction, the second on the confinement studies performed in the operating TJ-I Tokamak and the third one on the description of the physical properties of the soon to be started TJ-IU Torsatron.

DOE CLASIFICATION AND DESCRIPTORS: 700310, PLASMA CONFINEMENT, THERMONUCLEAR DEVICES, HELIAC STELLARATORS, TROSATRON STELLARATORS, TOKAMAK DEVICES, THERMONUCLEAR REACTIONS, THERMONUCLEAR REACTORS

CIEMAT - 723
Centro de Investigaciones Energéticas, Medioambientales y Tecnológicas
Instituto de Investigación Básica.- Madrid

Artículos Presentados a la 14ª CONFERENCIA INTERNACIONAL SOBRE FISICA DEL PLASMA Y FUSION NUCLEAR CONTROLADA

34 pp., 17 figs., 25 refs.

Este Informe contiene las contribuciones de la Unidad de Fusión del CIEMAT a la 14ª Conferencia Internacional sobre Física de Plasmas y Fusión Nuclear Controlada que, organizada por la Organización Internacional de la Energía Atómica, se celebró en Würzburg, Alemania, desde el 30 de Septiembre al 7 de Octubre de 1992. Tres artículos fueron presentados que resumían las principales líneas de trabajo realizadas en la Unidad durante los dos años anteriores: El primero sobre los avances teóricos en la comprensión del Heliac Flexible TJ-II en la construcción, el segundo sobre los estudios de confinamiento realizados en el Tokamak TJ-I actualmente en operación y el tercero sobre las propiedades físicas del Torsatron TJ-IU que pronto entrará en operación.

DOE CLASIFICATION AND DESCRIPTORS: 700310, PLASMA CONFINEMENT, THERMONUCLEAR DEVICES, HELIAC STELLARATORS, TROSATRON STELLARATORS, TOKAMAK DEVICES, THERMONUCLEAR REACTIONS, THERMONUCLEAR REACTORS

CIEMAT - 723
Centro de Investigaciones Energéticas, Medioambientales y Tecnológicas
Instituto de Investigación Básica.- Madrid

Artículos Presentados a la 14ª CONFERENCIA INTERNACIONAL SOBRE FISICA DEL PLASMA Y FUSION NUCLEAR CONTROLADA

34 pp., 17 figs., 25 refs.

Este Informe contiene las contribuciones de la Unidad de Fusión del CIEMAT a la 14ª Conferencia Internacional sobre Física de Plasmas y Fusión Nuclear Controlada que, organizada por la Organización Internacional de la Energía Atómica, se celebró en Würzburg, Alemania, desde el 30 de Septiembre al 7 de Octubre de 1992. Tres artículos fueron presentados que resumían las principales líneas de trabajo realizadas en la Unidad durante los dos años anteriores: El primero sobre los avances teóricos en la comprensión del Heliac Flexible TJ-II en la construcción, el segundo sobre los estudios de confinamiento realizados en el Tokamak TJ-I actualmente en operación y el tercero sobre las propiedades físicas del Torsatron TJ-IU que pronto entrará en operación.

DOE CLASIFICATION AND DESCRIPTORS: 700310, PLASMA CONFINEMENT, THERMONUCLEAR DEVICES, HELIAC STELLARATORS, TROSATRON STELLARATORS, TOKAMAK DEVICES, THERMONUCLEAR REACTIONS, THERMONUCLEAR REACTORS

CIEMAT - 723
Centro de Investigaciones Energéticas, Medioambientales y Tecnológicas
Instituto de Investigación Básica.- Madrid

Artículos Presentados a la 14ª CONFERENCIA INTERNACIONAL SOBRE FISICA DEL PLASMA Y FUSION NUCLEAR CONTROLADA

34 pp., 17 figs., 25 refs.

Este Informe contiene las contribuciones de la Unidad de Fusión del CIEMAT a la 14ª Conferencia Internacional sobre Física de Plasmas y Fusión Nuclear Controlada que, organizada por la Organización Internacional de la Energía Atómica, se celebró en Würzburg, Alemania, desde el 30 de Septiembre al 7 de Octubre de 1992. Tres artículos fueron presentados que resumían las principales líneas de trabajo realizadas en la Unidad durante los dos años anteriores: El primero sobre los avances teóricos en la comprensión del Heliac Flexible TJ-II en la construcción, el segundo sobre los estudios de confinamiento realizados en el Tokamak TJ-I actualmente en operación y el tercero sobre las propiedades físicas del Torsatron TJ-IU que pronto entrará en operación.

DOE CLASIFICATION AND DESCRIPTORS: 700310, PLASMA CONFINEMENT, THERMONUCLEAR DEVICES, HELIAC STELLARATORS, TROSATRON STELLARATORS, TOKAMAK DEVICES, THERMONUCLEAR REACTIONS, THERMONUCLEAR REACTORS

CIEMAT - 723
Centro de Investigaciones Energéticas, Medioambientales y Tecnológicas
Instituto de Investigación Básica.- Madrid

Artículos Presentados a la 14ª CONFERENCIA INTERNACIONAL SOBRE FISICA DEL PLASMA Y FUSION NUCLEAR CONTROLADA

34 pp., 17 figs., 25 refs.

Este Informe contiene las contribuciones de la Unidad de Fusión del CIEMAT a la 14ª Conferencia Internacional sobre Física de Plasmas y Fusión Nuclear Controlada que, organizada por la Organización Internacional de la Energía Atómica, se celebró en Würzburg, Alemania, desde el 30 de Septiembre al 7 de Octubre de 1992. Tres artículos fueron presentados que resumían las principales líneas de trabajo realizadas en la Unidad durante los dos años anteriores: El primero sobre los avances teóricos en la comprensión del Heliac Flexible TJ-II en la construcción, el segundo sobre los estudios de confinamiento realizados en el Tokamak TJ-I actualmente en operación y el tercero sobre las propiedades físicas del Torsatron TJ-IU que pronto entrará en operación.

DOE CLASIFICATION AND DESCRIPTORS: 700310, PLASMA CONFINEMENT, THERMONUCLEAR DEVICES, HELIAC STELLARATORS, TROSATRON STELLARATORS, TOKAMAK DEVICES, THERMONUCLEAR REACTIONS, THERMONUCLEAR REACTORS